Oldest proof of metal surface alteration? Characterization of Cu3As formation of prehistoric and recent Cu-As alloys

Surfaces and Interfaces 80 (2026) 108344

Contents lists available at ScienceDirect

Surfaces and Interfaces

journal homepage: www.sciencedirect.com/journal/surfaces-and-interfaces

Oldest proof of metal surface alteration? Characterization of Cu_3As formation of prehistoric and recent Cu-As alloys

Marianne Mödlinger [a,*], Elyse Canosa [b], Francisco Ardini [a], Giorgia Ghiara [c,*]

[a] Department of Chemistry, University of Genoa, Via Dodecaneso 31, 16146 Genoa, Italy
[b] Swedish National Heritage Board, Artillerigatan 33, 62138 Visby, Sweden
[c] DISAT, Politecnico di Torino, Corso Duca degli Abruzzi 24, 10129 Torino, Italy

ARTICLE INFO

Keywords:
Cu3As
Cu-As alloys
SEM-EDXS
XRD
ICP-AES
LOM

ABSTRACT

Arsenical copper artifacts from prehistory often display silvery Cu_3As surface layers whose origin has been debated for decades. To clarify the mechanisms, we reproduced the phenomenon experimentally by exposing Cu–As alloys (6–11 wt.% As) to acetic acid and vinegar–salt solutions, mimicking accessible prehistoric materials. Surface and microstructural characterization (LOM, SEM-EDXS, XRD) combined with ICP-AES analysis demonstrates that these conditions trigger selective copper leaching and progressive surface enrichment of Cu_3As. The resulting layers form banded morphologies with penetration depths up to 400 μm, closely resembling archaeological specimens, and enhance corrosion resistance. We introduce the term arsenification for this process of Cu_3As surface enrichment. Beyond providing insights into the earliest known case of intentional surface modification, these results establish a model for alloy surface engineering via controlled dealloying under mild acidic and saline conditions.

1. Introduction

Arsenical copper is the first intentionally produced human-made alloy, appearing in the archaeological record as early as c. 5000 BCE on the Iranian plateau, and later in Central Europe in the fourth and early third millennia BC [1–4]. As outlined in [2], more than 40 archaeological Cu-As objects with Cu_3As surface layers are currently known; most of them are weapons, of which more than 30 are daggers. They are found from Spain in the west to Palestine in the east and date from the Copper Age to the Late Bronze Age [5–8]. Surprisingly, all of these objects (tohugh containing far less than 15. wt.% As in the bulk) show at least partially a silvery surface, which is usually attributed to As concentrations in alloys greater than 15 wt. % As [9]. The silvery color derives from the formation of Cu_3As, containing about 29.5 wt. % As, and the ($\alpha + \gamma$)-eutectic, containing about 21 wt. % As [10–11]. According to the recrystallized (annealed) microstructure of the studied bronzes, these phases' formation could not have resulted from the casting process but took place afterward. It has been hypothesized that the silvery color slowly appears after long periods of internment or due to gradual phase changes that occur over thousands of years: for an overview on previous research see [2]. However, previous experiments have shown that the formation of Cu_3As on the object's surface presumably can also be triggered by depositing arsenical copper alloys in a sand and salt mixture for several months [8]. The reproduction of these experiments by the authors though remained without success. Further experiments have not yet been carried out with Cu-As alloys. Studies most similar to the one presented here, but with a different goal and on different alloys, include a study on the kinetics of growth and lateral spreading of an intermetallic layer along a free surface during the surface interdiffusion of $Cd_{21}Ni_5$ and Cu_5Zn_8 [12], the diffusion spreading of two intermetallic phases in the Cu-Sn system along a free surface [13], and the growth of Cu-Sn intermetallics at a pre-tinned copper-solder interface [14].

Archaeological references to similar techniques, but with different materials, are for instance known from pre-Hispanic Colombia and third millennium BCE Ur (depletion gilding [15–16]), or medieval Northern Europe and Roman "Corinthian" bronze (depletion silvering; [17–18]). Dezincification describes a similar, even though historically much younger process [19–20]. From a corrosion-science perspective, numerous studies have examined how specific environmental conditions can promote the preferential dissolution of one constituent of a metallic alloy through galvanic coupling and subsequent reprecipitation processes. In Cu–Al alloys [21] and Cu–Zn alloys [20,22–24] extensive work has demonstrated how microstructural heterogeneities and

* Corresponding authors.
E-mail addresses: marianne.moedlinger@edu.unige.it (M. Mödlinger), giorgia.ghiara@polito.it (G. Ghiara).

https://doi.org/10.1016/j.surfin.2025.108344
Received 1 September 2025; Received in revised form 10 December 2025; Accepted 17 December 2025
Available online 20 December 2025

phase-selective electrochemical responses lead to element-specific leaching, surface enrichment, and the formation of corrosion-derived layers with distinct chemical signatures. Comparable behaviors have also been observed under controlled chemical treatments, where selective etching conditions can reproduce similar dissolution–reprecipitation pathways [25]. In this paper we aim to determine, once and for all, the formation criteria for prehistoric silvery-surfaced arsenical copper alloys. To achieve this goal, the formation of Cu_3As on the sample's surface will be instigated through exposing different Cu-As alloys [26] to selected solutions also available during prehistory, which will infer whether prehistoric metalsmiths intentionally altered the surface of CuAs-objects to achieve a desired color, or whether it is the result of long-term changes to the alloy's phases. The alloy samples were then studied using electron microscopy (SEM-EDX), light optical microscopy (LOM), X-ray diffraction (XRD) and an inductively coupled plasma atomic emission spectrometer (ICP-AES). Further analyses using XPS (X-ray photoelectron spectroscopy) were planned, but unfortunately had to be postponed due to technical issues. The authors are, however, currently preparing a second paper on the topic, focusing on the formation mechanism of these Cu_3As features, which will include XPS analyses. This research has the potential to prove whether the surface of Cu-As alloys was deliberately silvery colored by depletion, which would be the oldest known evidence of such a process.

2. Methodology

2.1. Synthesis and sample preparation

Samples with a nominal composition Cu-As with 6, 8, and 11 wt. % As (for a total mass of 50 g each) were prepared by vapor-solid reaction between Cu and As. The starting metals used were Cu in small pieces (99.997 wt. % purity, Metallwerke Brixlegg, Brixlegg, Austria, MB-OF101 certified) and As in lumps (99.99 wt. % purity, Alfa Aesar, Haverhill, MA, USA). The elements were sealed inside a quartz tube under vacuum and slowly heated (in steps of 40 °C above 250 °C) until liquid (between 980–1030 °C). The samples were subsequently air-quenched. The as-cast samples were then cold rolled and reduced to about 80 % ("D" in sample name); a second set of samples ("R" in sample name) underwent additional annealing at 600 °C for 18 h with subsequent quenching in air. The samples' surfaces were then smoothed with up to 1000 grit. Table 1 provides information on the treatment of the samples in two different liquids: acetic acid (5 %; pH 2.5) and apple cider vinegar (5 %) + 1 M NaCl.

2.2. Optical microscopy

For microstructural analysis, cross-sections of each sample were mounted in cold epoxy resin and polished using 400–1200 SiC papers followed by a diamond suspension paste of up to 1 μm granulometry. The samples were characterized using optical microscopy in both bright and dark fields.

2.3. SEM-EDXS

Electron microscopy (SEM) was carried out at the Swedish National Heritage Board in Visby. Analyses were performed on the samples prepared for microstructural analysis (polished cross-sections) under high vacuum (less than 1 mPa) using a JEOL JSM-IT500 SEM with a tungsten hairpin filament. All imaging was executed using an objective lens aperture with a diameter of 30 μm and either a backscattered electron silicon P-N junction semiconductor detector under "composition" mode or secondary electron Everhart-Thornley detector. Elemental analysis was performed for quantitative and semi-quantitative chemical analysis, following gold coating of the samples using an X-ray radiation silicon drift detector with Peltier cooling. ZAF correction (as implemented in the JEOL software) was applied to the data, yielding reliable results for elements with atomic number $Z \geq 11$. Accelerating voltage for both imaging and EDS analysis ranged from 15 to 20 kV. Lighter elements, such as oxygen, and concentrations below 0.3 wt. % were considered semi-quantitative and reported only when clearly identifiable in the spectrum. Trace elements below the detection limit were excluded. Reported compositions represent the average of at least three measurements on non-corroded regions. Image analysis was performed at 200x magnification over 5 different areas of the samples with the Software Fiji-ImageJ, version 1.49b [27] to estimate the evolution of the volume percentage of the main phases (Cu(α) and Cu_3As) at the interface with the solution.

2.4. XRD

Powder X-ray diffraction (XRD) patterns were obtained for structural characterization using a Bruker D4 Endeavour diffractometer with Cu Kα radiation within a 2ϑ range of 5–100°, a step size of 0.02°, and a counting time of 4 or 6 s/step. Pure Si was utilized as an internal standard ($a = 5.4308(1)$ Å). Measurements were carried out directly on the sample surface. Samples were placed directly on a single-crystal Si zero background sample holder. Lazy Pulverix software [28] was used for pattern indexing.

Table 1
Treatment of the samples in different solutions for specific amounts of time (*R*=annealed; *D*=deformed; I or II indicates the series in the sample's name).

Series	solution	treatment samples	solution samples			metal sample names			
			5 weeks	10 weeks	16 weeks	5 weeks	10 weeks	16 weeks	
I	acetic acid (5 %)	CuAs-8	80 % def.	6 ml	6 ml	6 ml	I.8DA	I.8DAA	I.8DAAA
		CuAs-11	80 % def.	6 ml	6 ml	6 ml	I.11DA	I.11DAA	I.11DAAA
	apple cider vinegar (5 %) + 1 M NaCl	CuAs-8	80 % def.	6 ml	6 ml	6 ml	I.8DB	I.8DBB	I.8DBBB
		CuAs-11	80 % def.	6 ml	6 ml	6 ml	I.11DB	I.11DBB	I.11DBBB
Series	solution	treatment samples	solution samples			metal sample names			
			8 weeks	15 weeks	23 weeks	8 weeks	15 weeks	23 weeks	
II	acetic acid (5 %)	CuAs-6	80 % def.	10 ml	6 ml	10 ml	II.6DA		II.6DAAA
		CuAs-6	80 % def., annealed	10 ml	6 ml	10 ml	II.6R.A	II.6R.AA	II.6R.AAA
		CuAs-8	80 % def., annealed	10 ml	6 ml	10 ml	II.8R.A	II.8R.AA	II.8R.AAA
		CuAs-11	80 % def., annealed	10 ml	6 ml	10 ml	II.11R.A	II.11R.AA	II.11R.AAA
	apple cider vinegar (5 %) + 1 M NaCl	CuAs-6	80 % def.	10 ml	6 ml		II.6DB		II.6DBBB
		CuAs-6	80 % def., annealed	10 ml	6 ml	10 ml	II.6R.B	II.6R.BB	II.6R.BBB
		CuAs-8	80 % def., annealed	10 ml	6 ml	10 ml	II.8R.B	II.8R.BB	II.8R.BBB
		CuAs-11	80 % def., annealed	10 ml	6 ml	10 ml	II.11R.B	II.11R.BB	II.11R.BBB

2.5. ICP-AES

The inductively coupled plasma atomic emission spectrometer (ICP-AES) used was an axially-viewed Varian (Springvale, Australia) Vista PRO. The sample introduction system consisted of a glass concentric K-style pneumatic nebulizer joined to a glass cyclonic spray chamber (both from Varian). The main operating conditions are listed in Table S1. Ultrapure water for the dilution of the samples and preparation of the standards was supplied by the four-column ion-exchange system Milli-Q fed by the reverse osmosis system Elix 3, both from Merck Millipore (Burlington, MA, USA). Single-element standard solutions (1000 mg/L) of As and Cu were obtained from Sigma-Aldrich (St. Louis, MO, USA) and Merck. Suprapur grade nitric acid (65 %) was provided by VWR International (Leuven, Belgium). Samples were properly diluted (2–100 fold) and analyzed by ICP-AES, using Lu (c = 10 mg/l) as an internal standard to compensate for the physical interferences and instrumental drift. A 5-point calibration curve was built (0–5 mg/l for As, 0–200 mg/l for Cu), with an obtained R^2>0.999 for all the selected wavelengths. The standard solutions were prepared in 1 % (v/v) nitric acid by proper dilution with ultrapure water.

3. Results and discussion

3.1. Microstructural analyses (LOM)

The as-cast and 80 % deformed samples still show Cu_3As and (α+γ) eutectic deriving from the casting, as well as deformed dendritic structures. After exposure of the samples to various solutions, new banded Cu_3As formed, particularly on and near the surface of the samples directly exposed to the solutions:

The exposure of deformed samples to acetic acid for 5 weeks resulted in the first formation of banded Cu_3As on the sample I.8DA, whereas nothing was observed on sample I.11DA; the process seemed to start after 5 weeks of exposure (see sample I.11DAA). Sample II.6DA instead contains Cu_3As and (α+γ) eutectic from the casting process even after 8 weeks of exposure; no new formation of banded Cu_3As was observed. After 15 weeks, the formation of banded Cu_3As was significantly increased (samples I.8DAAA and I.11DAAA), or started after 15 weeks (sample II.6DAAA). For the apple cider vinegar solution on deformed samples, this was first observed on sample I.11DB after 5 weeks of exposure. After 10 weeks of exposure, the sample I.8DBB also showed the first signs of band-like Cu_3As formation on and near the surface of the sample. Sample II.6DB, on the other hand, was found to have a sponge-like structure after 8 weeks due to Cu depletion, with the newly formed small Cu_3As bands remaining. After 16 weeks of exposure, the formation of such Cu_3As bands was significantly increased in both I.8DBBB and I.11DBBB samples. Sample II.6DBBB also showed a significant increase in banded Cu_3As after 23 weeks, forming a sponge-like Cu_3As structure on the surface, possibly due to a selective dissolution of the Cu(α) matrix.

However, the formation of banded Cu_3As was different in the samples that were also subsequently annealed at 600 °C for about 18 h (most of Series II samples). In particular, the Cu_3As and (α+γ) eutectic still present in the as-cast, deformed samples disappeared during annealing, with only small areas of (α+γ) eutectic remaining on some samples. However, all samples showed the formation of Cu_3As along the grain boundaries (as seen also via SEM-EDXS; Fig. 2) close to and partially on the sample surface after 8 weeks of exposure to both acetic acid and apple cider vinegar.

For each nominal alloy composition (CuAs-6, CuAs-8, and CuAs-11) and corrosion condition (5 % acetic acid and 5 % apple vinegar containing 1 M NaCl), surface enrichment of the Cu_3As phase was observed to occur preferentially along the grain boundaries. This phenomenon was especially evident in the annealed samples, where the grain boundaries displayed the characteristic polygonal morphology typical of recrystallized copper alloys. For the as-cast and deformed samples, an expansion of the already present Cu3As present in the interdendritic regions is mainly observed. The "arsenification" process—defined here as the progressive surface enrichment and inward growth of the Cu_3As phase—proceeded over time, with penetration depths varying based on alloy composition, thermal treatment, and the specific corrosive medium. Notably, the formation of banded Cu_3As structures, similar to those identified in archaeological artifacts [2–8], was significantly more pronounced in samples exposed to apple cider vinegar. In these cases, thicker Cu_3As bands developed, with final penetration depths ranging from 100 to 400 μm in the as-cast and deformed alloys, and from 300 to 400 μm in the annealed ones—up to twice the depth observed under acetic acid exposure.

Concerning the as-cast and deformed samples, the Cu_3As superficial layer is denser, and thicker bands form along the direction of deformation (cold lamination). These bands start at the Cu_3As interdendritic regions from the original as-cast (dendritic structure) and accumulate dense layers of Cu_3As close to the surface. This leads to a higher volume fraction of Cu_3As on the surface of the actual metal sample (not the surface of the cross-section) compared to the surface of the recrystallized samples. See Fig. 1.

3.2. SEM-EDXS

SEM-EDXS analysis confirmed the LOM observations: only Cu(α), Cu_3As, and (α+γ) eutectic of the Cu-As binary system were observed. In addition, a gradual increase of As was detected towards the formation of the newly formed Cu_3As bands. Fig. 4 and Fig. S2 and S3 show how the alloy interfaces evolve with the solution at the selected time points and alloy compositions (CuAs-6, CuAs-8, and CuAs-11), as well as the thermomechanical treatments (as-cast and deformed or annealed) and solutions (A and B). BSE observations detected a compositional gradient, more pronounced on the surface in contact with the solution, compared to the bulk. Point and area elemental analysis (EDXS) confirmed the detection of the Cu_3As phase on the surface of each alloy.

Fig. 5a and 5b display the As wt. % calculated from the average of the measurements of the Cu_3As phase for CuAs-6 and CuAs-11 for each solution (acetic acid and apple cider vinegar with salt) together with the nominal Cu_3As composition (29.1 to 32.5 As wt. %) taken from the Cu-As phase diagram (dotted lines) [26]. Figs. S3a and S3b, supplementary material, also displays the As wt. % calculated for CuAs-8. The As wt. % in the Cu_3As phase remains constant throughout the test for each alloy, slightly above the nominal concentration of the intermetallic phase, which is compatible with the instrumental error of the EDXS analysis. A lower amount of As (from 26.5 ± 4.9 to 28.4 ± 2.3 As wt. %) was detected in annealed CuAs-6 samples of series II (II.6R.A to II.6R.AAA) immersed in acetic acid and in the CuAs-8 sample of series I and II (I.8DA to I.8DAAA and II.8R.B to II.8R.BBB) possibly due to the interaction volume of the SEM beam averaging the signal related to the Cu_3As phase and the Cu(α) matrix. Interestingly, while the As wt. % in the Cu(α) remained stable across all experiments for the annealed alloys, noticeable variations in As concentration were observed in the matrix of the as-cast and later deformed samples. However, these fluctuations can be attributed to the compositional heterogeneity introduced during the initial casting process. This heterogeneity, clearly evidenced by SEM-BSE imaging (Fig. 4), resulted in regions with varying As content within the Cu(α) solid solution. Therefore, when considering the average As concentration across both As-rich and As-poor regions of the Cu(α) matrix, these apparent modifications in As wt. % can be regarded as insignificant.

Image analysis was conducted to quantify the volume fractions of all identified phases and to evaluate the influence of solution type on the surface enrichment of the Cu_3As phase. As shown in Fig. 6 and Fig. S4c and S4d (supplementary material), both the Cu_3As phase and the Cu(α) matrix were examined at selected time intervals to track their evolution throughout the experiment. The quantitative data were derived from a representative number of measurements—at least five distinct areas on

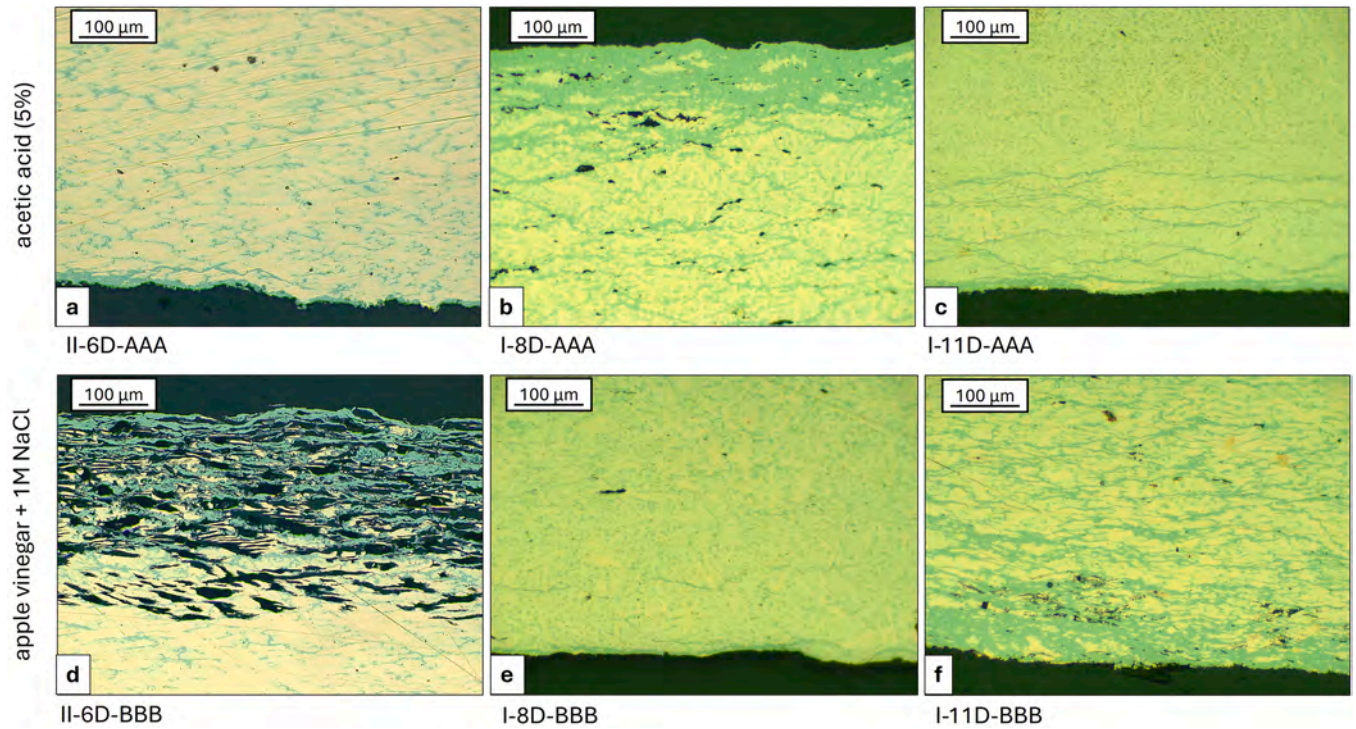

Fig. 1. Cu-As samples exposed to different liquids. Before exposure, all samples were cast and 80 % deformed (via rolling). Formation of banded Cu_3As: a) 40 µm; b) 160 µm; c) 180 µm; d) 230 µm; e) 100 µm; f) 400 µm. Exposure time: a) 23 weeks; b) and c): 16 weeks; d) 23 weeks; e) and f): 16 weeks.

each sample—captured at 200x magnification. Consequently, the reported volume fractions correspond specifically to the surface layer within the first 200 µm of depth from the exposed surface. The exposure to both acetic acid and apple cider vinegar solutions containing 1 M NaCl clearly promotes the surface enrichment of Cu_3As across all as-cast and deformed alloys (CuAs-6D, CuAs-8D, and CuAs-11D, Figs. 6a, 6b, S4c and S4d). This enrichment follows a non-linear trend, gradually increasing over time and reaching its maximum by the end of the experiment. Although the penetration depth of the Cu_3As phase is consistently lower in samples treated with acetic acid compared to those exposed to apple cider vinegar, the resulting Cu_3As layer is notably more homogeneous and compact. In particular, in acetic acid, within the first 200 µm from the surface, the Cu_3As volume fraction reaches 14.2 ± 2.6 % for CuAs-6, 37.4 ± 8.7 % for CuAs-8 and 29.6 ± 1.1 % for CuAs-11, indicating a substantial and uniform enrichment of the phase on the surface of the alloy under these conditions. The relative difference in Cu_3As volume fraction among the alloys could possibly be attributed to the initial higher As wt. % that could possibly allow for a more rapid copper depletion from the surface. In comparison, slightly lower volume fractions of Cu_3As were measured in the as-cast alloys exposed to the apple cider vinegar solution, with values of 12.4 ± 4.6 % for CuAs-6, 10.6 ± 1.9 for CuAs-8 and 19.8 ± 5.0 % for CuAs-11. This suggests that, although both solutions promote surface enrichment, acetic acid may be more effective in generating a thicker and more compact Cu_3As layer under the given experimental conditions.

In contrast, both solutions appear less effective for the annealed alloys (CuAs-6R, CuAs-8R, and CuAs-11R). Although these alloys exhibit greater penetration depths of the Cu_3As phase, the enrichment remains largely confined to the grain boundaries and does not extend significantly into the grain core. As a result, surface enrichment in these annealed alloys progresses at a much slower rate, with final Cu_3As volume fractions remaining below 6 % for samples II.6R.AAA, II.8R.AAA II.11R.AAA and II.6R.BBB (confirmed also by XRD analyses; see below). An exception to this trend is observed in the CuAs-8R and CuAs-11R alloys immersed in apple cider vinegar, which displays a marked increase in Cu_3As formation starting from 15 to 23 weeks of exposure. In this case, the volume fraction rises sharply to 9.4 ± 0.5 % and 12.9 ± 1.5 %, indicating a distinct acceleration of the "arsenification" process under this specific set of conditions.

3.3. XRD

The XRD patterns of the surface measurements of the CuAs-sheets, Fig. 7 and Fig. S5 (supplementary material) for the as cast and deformed samples (annealed samples not visible due to the very low amount of Cu_3As on the superficial layer of the alloys), confirm previous observations from LOM and SEM-EDXS analysis, showing that the samples consist of Cu(α) and Cu_3As only [11]. However, Cu_2O peaks were also observed in the samples exposed to 5 % acetic acid for each alloy (for CuAs-8 see supplementary material). While not quantitatively measurable, a qualitative increase in Cu_3As on the surface of the samples after exposure to both solutions is clearly evident. This is particularly evident in the samples exposed to 5 % acetic acid (see Fig. 4 for the as-cast and deformed samples). The same trend, though less intense, is also evident in the annealed samples. This can easily be explained by observing the differences in the formation of Cu_3As on as-cast and deformed samples compared with annealed samples (see Figs. 1 and 2). While the Cu_3As concentration is preferentially located at the surface of the as-cast and deformed samples, it extends deeper into the core of the annealed samples along the grain boundaries, leading to a lower Cu_3As concentration at the surface.

3.4. ICP-AES

To assess the impact of the solution (acetic acid or vinegar and 1 M NaCl) on the arsenification process, solution samples were extracted from the test environment at the conclusion of the experiment, and the ionic release of both copper (Cu) and arsenic (As) into the solution was quantitatively measured using inductively coupled plasma atomic emission spectroscopy (ICP-AES). This analysis provided insight into the extent of metal dissolution and surface transformation driven by each corrosive medium. Results are displayed in Fig. 8 and Fig. S6

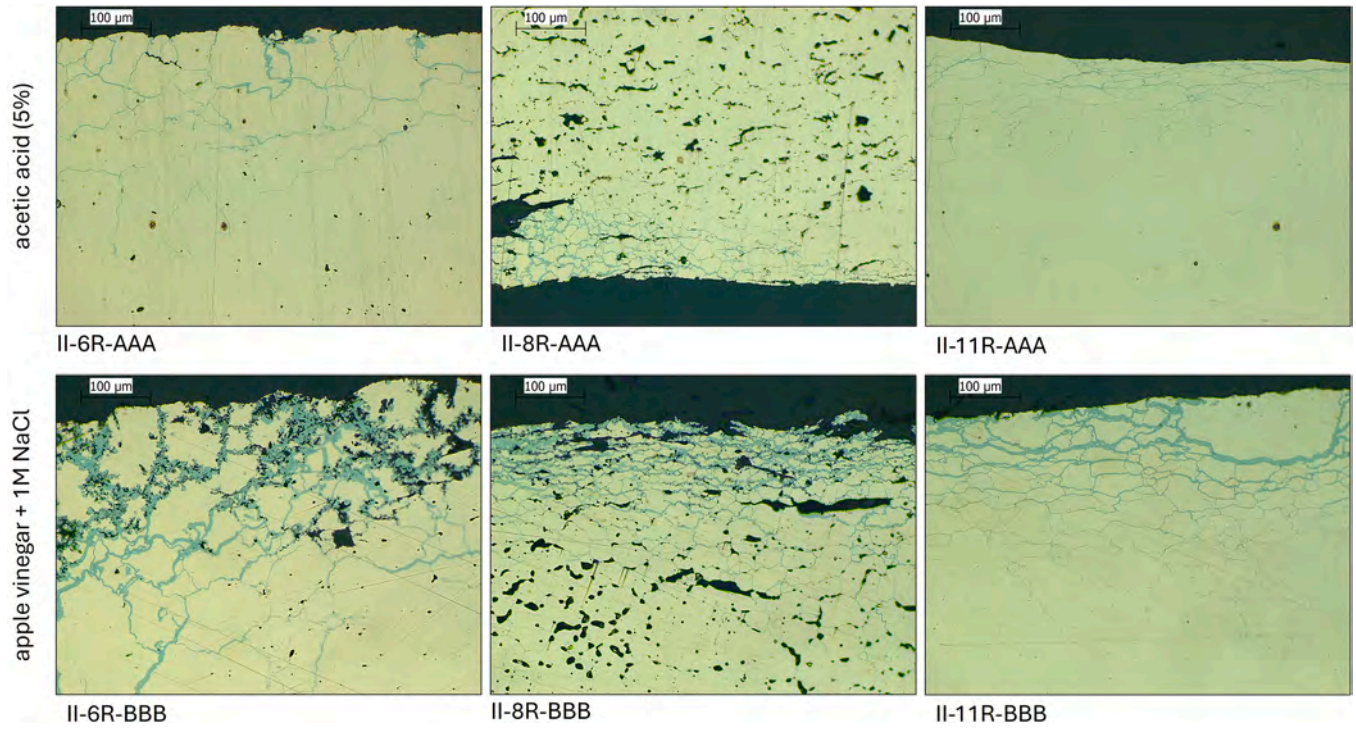

Fig. 2. Cu-As samples exposed to different liquids. Before exposure, all samples were cast, 80 % deformed (via rolling) and subsequently annealed at 600 °C for a duration of 18 h, followed by air quenching. Depth of the formation of Cu_3As along the grain boundaries: a) 250 µm; b) 120 µm; c) 200 µm; d) 400 µm; e) 300 µm; f) 300 µm. Exposure time all samples: 23 weeks.

(supplementary material). Copper dissolution was observed in both the acetic acid and apple cider vinegar solutions, indicating that both environments actively promote corrosion. In addition, the effect seemed to be generally more pronounced for the CuAs-8 and CuAs-11 alloys, which exhibit comparable behavior (Fig. S6). In the presence of acetic acid, this reaction is thermodynamically favorable only when oxidized copper species—specifically Cu_2O or CuO—are detected. They then react with acetic acid to form soluble copper complexes [29–30]. XRD analysis supported this mechanism, revealing small but distinct peaks corresponding to Cu_2O on the surfaces of all tested alloys after 5 or 8 weeks of exposure to acetic acid (see Fig. 7a and 7c Fig. S5 supplementary material). These findings confirm the role of Cu oxidation in initiating the dissolution process. Notably, the highest levels of copper release were recorded in the samples exposed to apple cider vinegar in the presence of 1 M NaCl (up to 600 mg in 200 mL of solution), with concentrations reaching up to six times those measured in the acetic acid solutions. This enhanced dissolution may be attributed to the formation of less stable copper compounds, promoted by the combined action of chloride ions and acetate ions in solution. The presence of chlorides likely intensifies surface interactions, accelerating the breakdown of the protective oxide layer and synergistically increasing copper solubility [31].

The release of As generally follows the same trend observed for Cu, though the absolute quantities detected in solution are significantly lower. In the case of acetic acid, the impact on arsenic dissolution is minimal, with ionic release ranging from 0.300 to 0.600 mg per 200 mL of solution. A slightly higher amount of As in the solution is noted for the CuAs-6 alloy, which could indicate a higher reactivity of the material towards the solution. Overall, these values suggest that acetic acid exerts only a limited influence on the dissolution of arsenic from the alloy surface. In contrast, a markedly different behavior is observed in samples exposed to apple vinegar combined with 1 M NaCl. Here, thermomechanical treatment appears to play a more significant role in influencing arsenic release. Although still limited in magnitude, the CuAs-6 and CuAs-11 as-cast alloys exhibit a noticeably higher ionic release, with values ranging between 1.0 and 2.5 mg per 200 mL of solution. In comparison, all annealed alloys (CuAs-6, CuAs-8 and CuAs-11) release only negligible amounts of As, underscoring the influence of microstructural features—such as grain boundary density and phase distribution—on the corrosion-driven dissolution of this element.

4. Conclusions

The presence of Cu_3As layers on the surface of Copper and Bronze Age objects, most of them weapons, provides a first indication that the silvery colored layers were intentionally produced, as they are not found on other objects with similar chemical composition, thermomechanical treatment, age, and/or find context. Moreover, as all archaeological objects with a Cu_3As surface layer show a (deformed and) recrystallized microstructure, this layer cannot be the result of segregation during the cooling process immediately after casting. Consequently, the formation of Cu_3As must have occurred after the final thermomechanical treatment. One of the easiest and, according to the similarity of the microstructural features in the samples produced by the authors, most likely way to produce a Cu_3As surface layer (as well as the inner structural changes) is through human-induced copper depletion possibly through a specific superficial treatment. Such a process could have been achievable even in prehistoric times using accessible materials such as acetic acid, apple cider vinegar, and salt. These solutions have proven highly effective in promoting the arsenification process, defined here as the surface enrichment in the Cu_3As phase, resulting from selective copper leaching from the alloy. This intentional surface modification can be considered among the earliest known techniques for altering the appearance of metal objects—specifically to change their color—excluding practices of artificial patination. The resulting Cu_3As layer, often forming in wavy or banded patterns on the alloy surface, closely resembles structures observed in archaeological arsenical bronze artifacts. The detailed formation mechanism of these Cu_3As features, and their significance in archaeological metallurgy, will be explored in a separate publication.

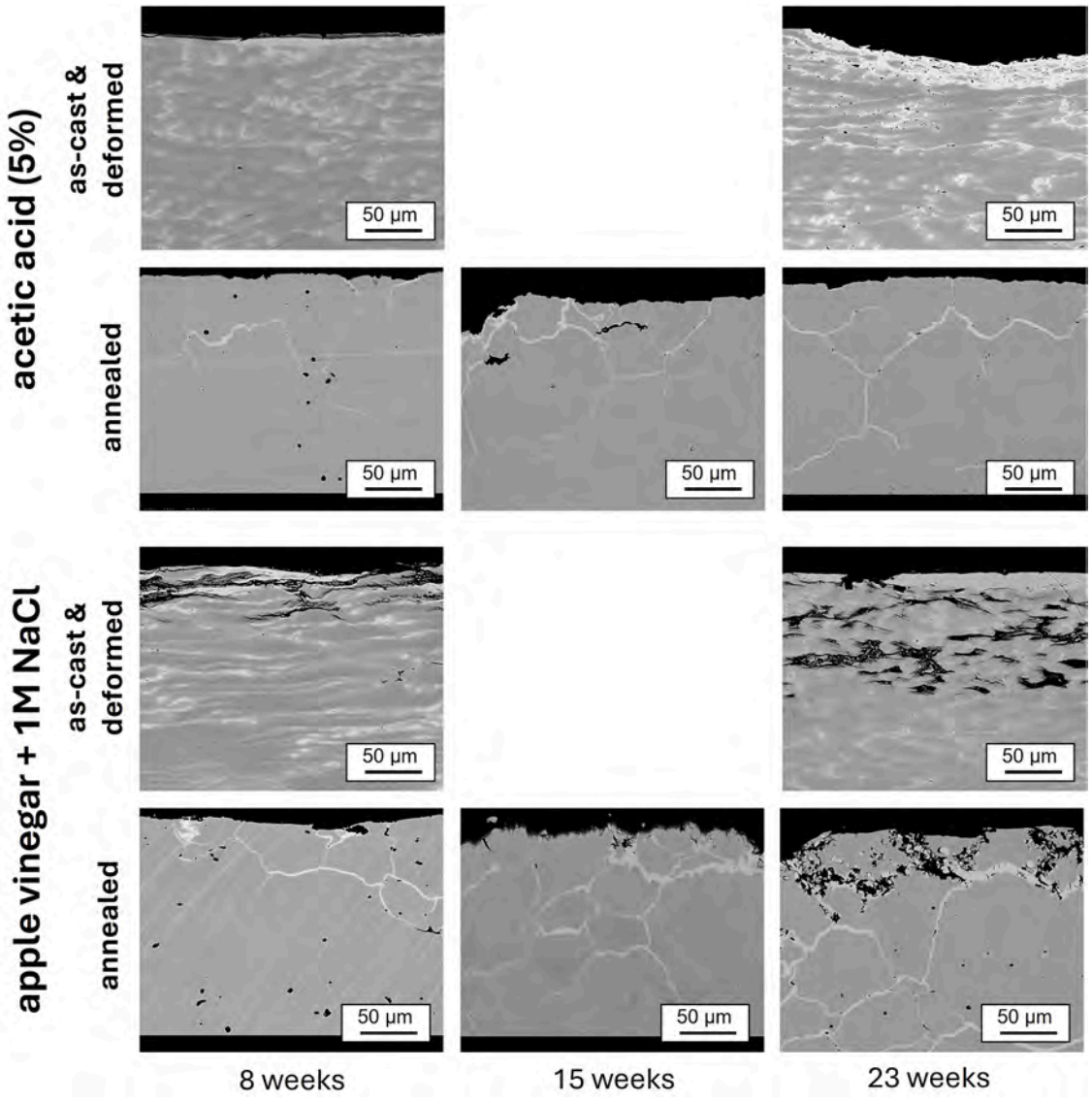

Fig. 4. SEM-images of CuAs-11 samples exposed to different liquids. The SEM-images of CuAs-6 and CuAs-8 alloys can be found as Supplementary Files S2 and S3.

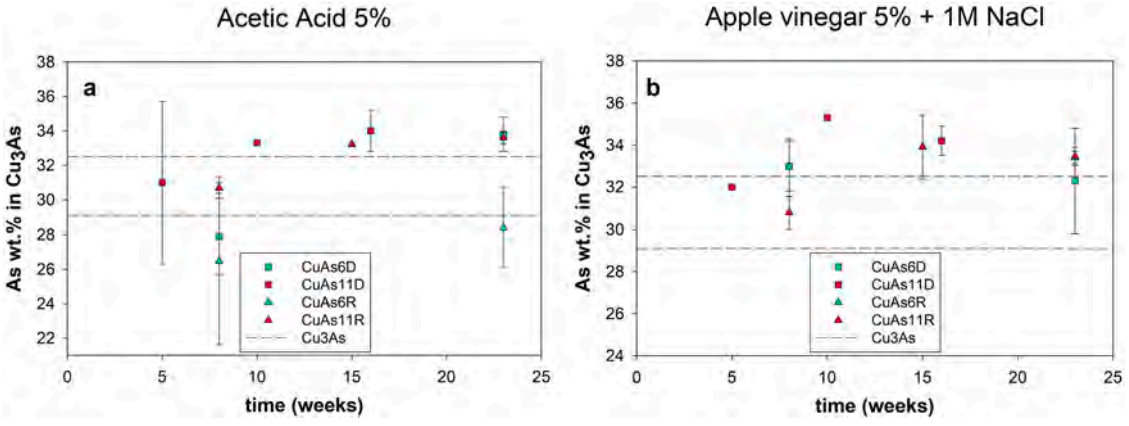

Fig. 5. Arsenic wt. % evolution on the main phases of the alloys: a) Cu_3As composition for alloy CuAs-6 and CuAs-11 in solution A (acetic acid 5 %); b) Cu_3As composition for alloys CuAs-6 and CuAs-11 in solution B (apple cider vinegar (5 %) and 1 M NaCl). *D*=as cast and deformed, *R*=annealed.

Funding

This research was funded by the European Union's Horizon 2020 research and innovation program under the Marie Skłodowska-Curie by the grant agreement No [101,018,804]. Financial support by the Access to Research Infrastructures activity (Swedish National Heritage Board)

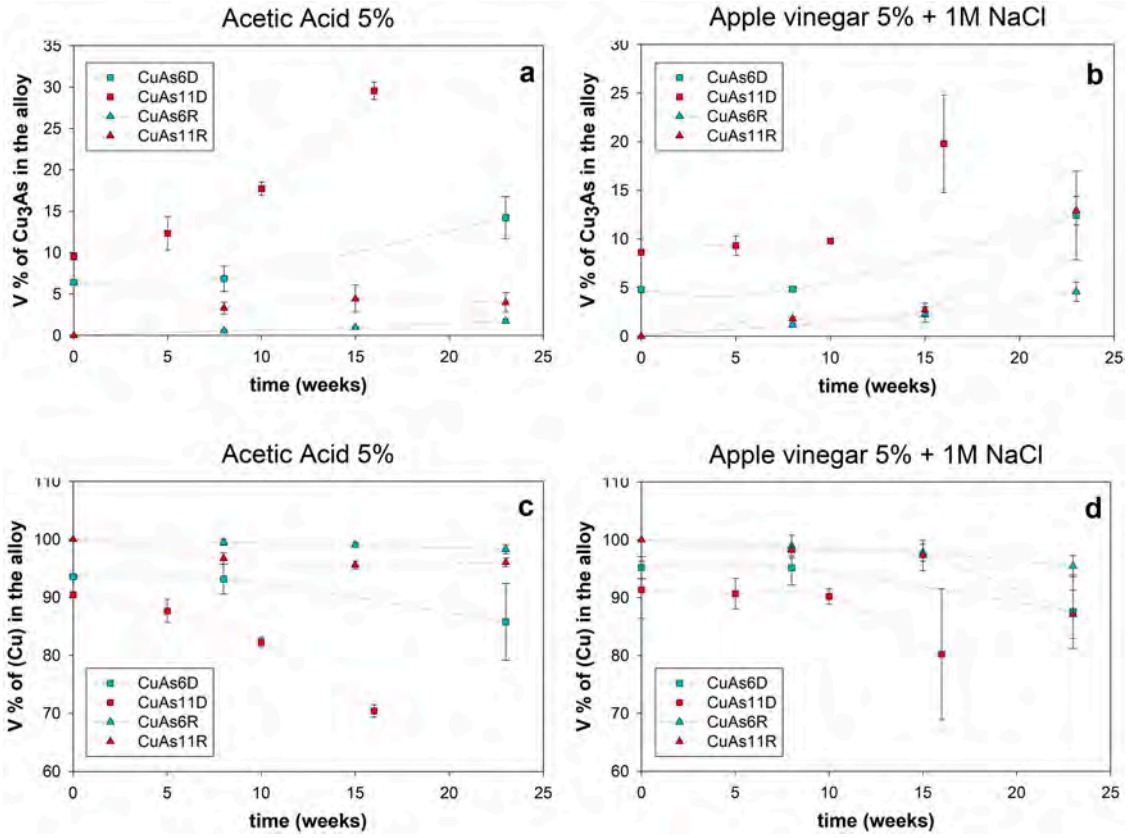

Fig. 6. Volume percentage trend on the main phases of the alloys: a) Cu_3As volume fraction variation for alloys CuAs-6 and CuAs-11 in solution A (acetic acid 5 %); b) Cu_3As volume fraction variation for alloys CuAs-6 and CuAs-11 in solution B (apple vinegar (5 %) and 1 M NaCl); c) Cu(α) volume fraction variation for alloys CuAs-6 and CuAs-11 in solution A; d) Cu(α) volume fraction variation for alloys CuAs-6 and CuAs-11 in solution B. *D*=as-cast and deformed, *R*=annealed.

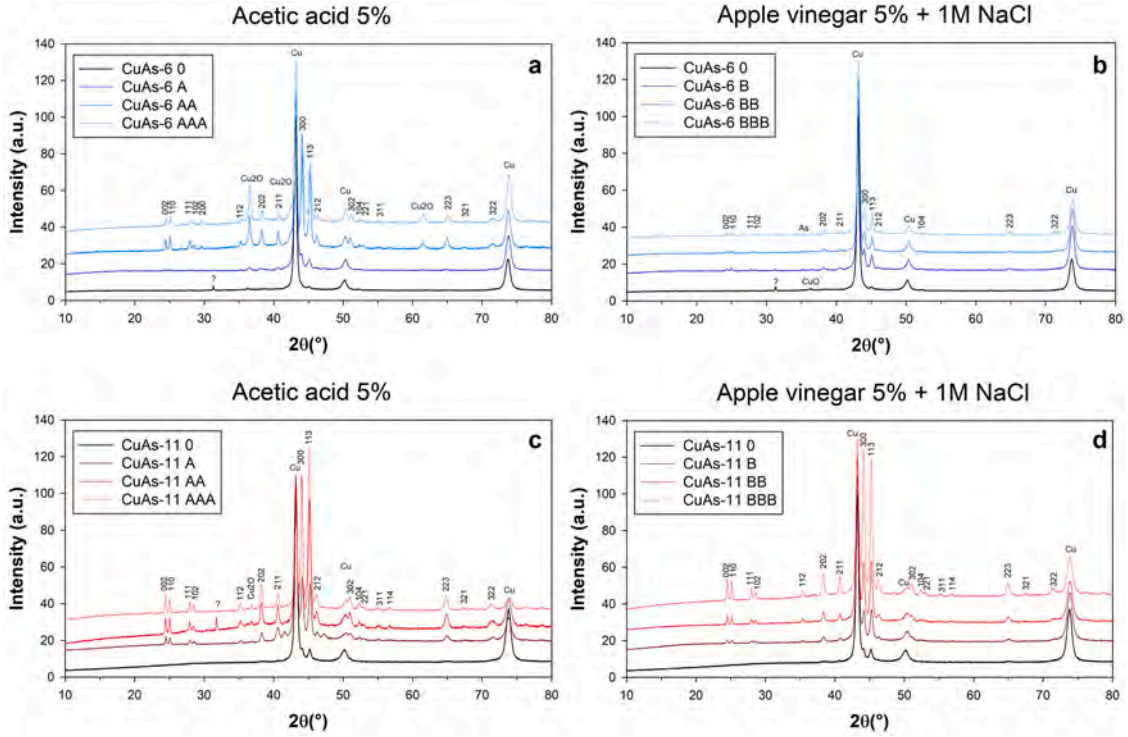

Fig. 7. Comparison of the XRD patterns from the surface of as-cast and deformed CuAs sheets after exposure to 5 % acetic acid (a and c) and 5 % apple vinegar + 1 M NaCl (b and d). The top row shows a comparison of the XRD patterns of CuAs-6 samples after exposure to the solutions for different times. The bottom row shows a comparison of the XRD patterns of CuAs-11 samples after exposure to the solutions for different times.

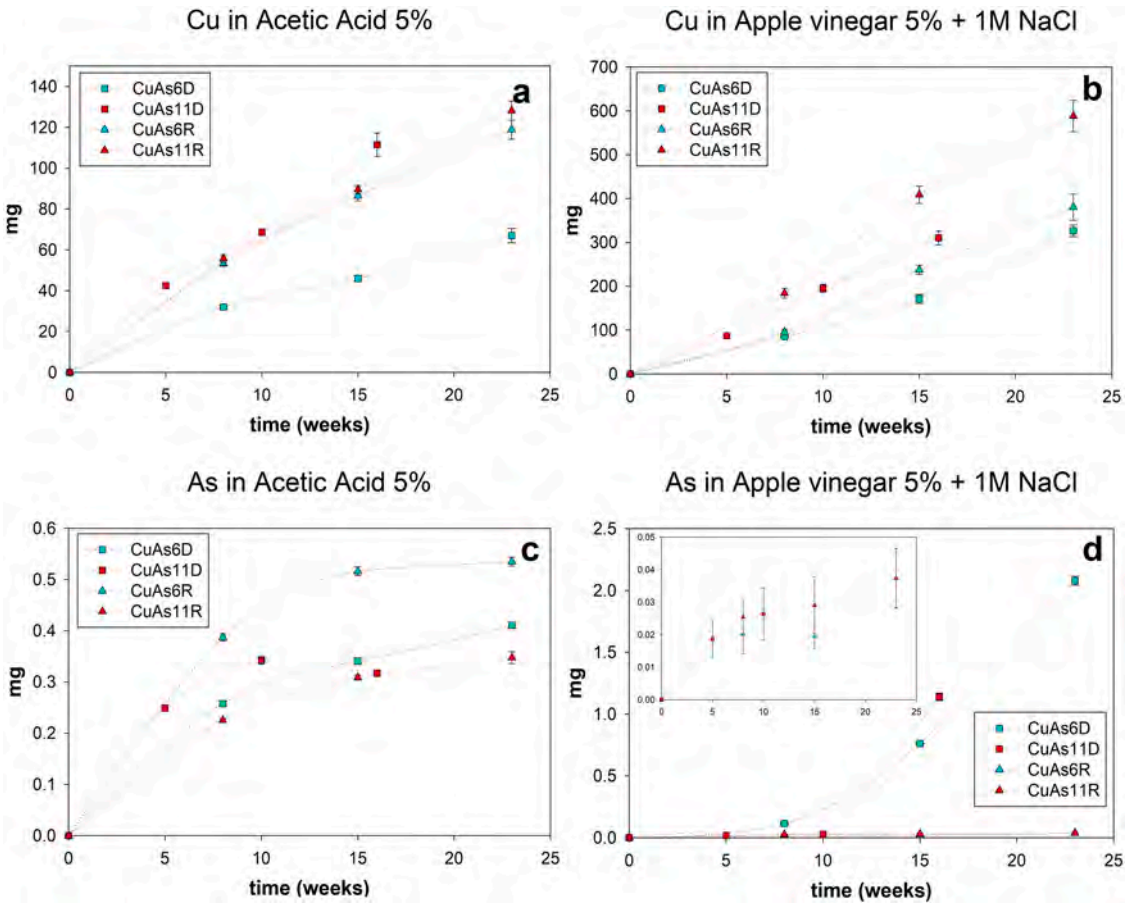

Fig. 8. Ionic release in solution of Cu and As. a) Cu release for alloys CuAs-6 and CuAs-11 in solution A (acetic acid 5 %); b) Cu release for alloys CuAs-6 and CuAs-11 in solution B (apple cider vinegar (5 %) and 1 M NaCl); c) As release for alloys CuAs-6 and CuAs-11 in solution B; d) As release for alloys CuAs-6 and CuAs-11 in solution B. *D*=as cast and deformed, *R*=annealed.

in the Horizon 2020 Programme of the EU (IPERION HS Grant Agreement n.871034) is gratefully acknowledged.

CRediT authorship contribution statement

Marianne Mödlinger: Writing – review & editing, Writing – original draft, Visualization, Validation, Methodology, Investigation, Formal analysis, Data curation. **Elyse Canosa:** Writing – review & editing, Investigation, Formal analysis. **Francisco Ardini:** Writing – review & editing, Writing – original draft, Investigation, Formal analysis. **Giorgia Ghiara:** Writing – review & editing, Writing – original draft, Visualization, Validation, Methodology, Investigation, Formal analysis, Data curation.

Declaration of competing interest

The authors declare that they have no known competing financial interests or personal relationships that could have appeared to influence the work reported in this paper.

Supplementary materials

Supplementary material associated with this article can be found, in the online version, at doi:10.1016/j.surfin.2025.108344.

Data availability

Data will be made available on request.

References

[1] D. Berger, Bronzezeitliche Färbetechniken an Metallobjekten nördlich der Alpen. Eine archäometallurgische Studie zur prähistorischen Anwendung von Tauschierung und Patinierung anhand von Artefakten und Experimenten. Forschungsberichte Des Landesmuseums Für Vorgeschichte Halle 2 (Halle/Saale, Landesamt für Denkmalpflege Und Archäologie Sachsen-Anhalt, 2012.

[2] M. Mödlinger, B. Sabatini, A *Re*-evaluation of inverse segregation in prehistoric Cu-As objects, J. Archaeol. Sci. 74 (2016) 60–74, https://doi.org/10.1016/j.jas.2016.08.005.

[3] S. Shalev, P. Northover, The metallurgy of the Nahal Mishmar Hoard reconsidered, Archaeometry. 35 (2007) 35–47, https://doi.org/10.1111/j.1475-4754.1993.tb01022.x.

[4] Northover, J.P., Anschnitt beih 8 (1998) 113–121.

[5] M. Mödlinger, B. Sabatini, Bronze age caucasian metalwork: alloy choice and combination, J. Archaeol. Sci.: Rep. 16 (2017) 248–257, https://doi.org/10.1016/j.jasrep.2017.10.018.

[6] M. Bernabale, F. Cognigni, F. Mura, L. Nigro, D. Montanari, M. Rossi, V. De, C. 3D imaging of micro-segregation and corrosion behavior of alloying elements in archaeological artefacts from Motya (Sicily, Italy), Corros. Sci. 211 (2023), https://doi.org/10.1016/j.corsci.2022.110900.

[7] N. Meeks, Surface characterization of tinned bronze, high-tin bronze, tinned iron and arsenical bronze, in: S. La Niece, P. Craddock (Eds.), Metal Plating and Patination, Butterworth-Heinemann, 1993, pp. 247–275, https://doi.org/10.1016/B978-0-7506-1611-9.50025-X.

[8] N.V. Ryndina, I.G. Ravich, Silver arsenic coatings on products of the Maikop culture (according to laboratory modeling), Br. Commun. Inst. Archaeol. 237 (2015) 90–103. = и. Г. равич, н. в. рындина. СеребриСтые МыШьяковые покрытия на иЗделиях МайкопСкой культуры, Краткие сообщения Института археологии 237, 2015, 90–103.].

[9] M. Mödlinger, D. Macció, B. Sabatini, A. Cziegler, H. Schnideritsch, Archaeological arsenical bronzes: constantly out-of-equilibrium, Metall. Mater. Trans. B 49 (2018) 2505–2513, https://doi.org/10.1007/s11663-018-1322-8.

[10] M. Mödlinger, M. Kuijpers, D. Braekmans, D. Berger, Quantitative comparisons of the color of CuAs, CuSn, CuNi, and CuSb alloys, J. Archaeol. Sci. 88 (2017) 14–23, https://doi.org/10.1016/j.jas.2017.09.001.

[11] M. Mödlinger, A. Provino, P. Solokha, F. Caglieris, M. Ceccardi, D. Macciò, M. Pani, C. Bernini, D. Cavallo, A. Ciccioli, P. Manfrinetti, Cu3As: uncommon crystallographic features, low-temperature phase transitions, thermodynamic and physical properties, Materials 16 (6) (2023) 2501, https://doi.org/10.3390/ma16062501.
[12] Y.S. Kaganovskii, L.N. Paritskaya, V.V. Bogdanov, Kinetics and mechanisms of intermetallic growth by surface interdiffusion, MRS Online Proc. Libr. 527 (1998) 303–307, in: https://link.springer.com/article/10.1557/PROC-527-303.
[13] Yu. Kaganovskii, L.N. Paritskaya, V.V. Bogdanov, Lateral diffusion spreading of two competitive intermetallic phases along free surface (System Cu-Sn), J. Basic Princ. Diffus. Theory Exp. Appl. (2008). https://d-nb.info/1240315392/34.
[14] A.J. Sunwoo, J.W. Morris, G.K. Lucey, The growth of Cu-Sn intermetallics at a pretinned copper-solder interface, Met. Trans. A 23 (1992) 1323–1332, https://doi.org/10.1007/BF02665064.
[15] J. Sáenz-Samper, M. Martinón-Torres, Depletion gilding, innovation and life-histories: the changing colours of Nahuange metalwork, Antiquity. 91 (359) (2017) 1253–1267, https://doi.org/10.15184/aqy.2017.97.
[16] S.L. Niece, Depletion gilding from third millennium BC Ur, Iraq. 57 (1995) 41–47, https://doi.org/10.2307/4200400.
[17] S.W. Merkel, Silver and the silver economy at Hedeby (Verlag Marie Leidorf, Bochum (2016).
[18] D.M. Jacobson, Corinthian bronze and the gold of the alchemists, Gold. Bull. 33 (2000) 60–66, https://doi.org/10.1007/BF03216582.
[19] Zhou, Y., Mahmood, S., Engelberg, D.L. Brass dezincification with a bipolar electrochemistry technique, surfaces and interfaces 22, 2021, 100865. https://doi.org/10.1016/j.surfin.2020.100865.
[20] V.F. Lucey, The mechanism of dezincification and the effect of arsenic. I, Br. Corros. J. 1 (1) (1965) 9–14, https://doi.org/10.1179/000705965798328254.
[21] A. El Warraky, A. El-Aziz, K. Soliman, Copper redeposition and surface enrichment during the dissolution of Al-Cu alloys in different concentrations of NaCl solution. Part 1 – electrochemical measurements, Anti-Corros. Methods Mater. 54 (3) (2007) 155–162, https://doi.org/10.1108/00035590710748623. No.
[22] F. Robinson, M. Shalit, The dezincification of brass, Corros. Technol. 11 (4) (1964) 11–14, https://doi.org/10.1108/eb020168.
[23] V.F. Lucey, The mechanism of dezincification and the effect of arsenic. II, Br. Corros. J. 1 (2) (1965) 53–59, https://doi.org/10.1179/000705965798328137.
[24] A.P. Pchelnikov, A.D. Sitnikov, I.K. Marshakov, V.V. Losev, A study of the kinetics and mechanism of brass dezincification by radiotracer and electrochemical methods, Electrochim. Acta 26 (5) (1981) 591–600, https://doi.org/10.1016/0013-4686(81)80025-4.
[25] C. Trinidad, J. Światowska, S. Zanna, A. Seyeux, D. Mercier, et al., Effect of surface preparation treatments on copper enrichment on 2024 aluminium alloy surface, Appl. Surf. Sci. 560 (2021) 149991 ff10.1016/j.apsusc.2021.149991.
[26] P.R. Subramanian, D.E. Laughlin, The As−Cu (Arsenic-Copper) system, Bull. Alloy Ph. Diagr. 9 (1988) 605–618, https://doi.org/10.1007/BF02881964.
[27] J. Schindelin, I. Arganda-Carreras, E. Frise, et al., Fiji: an open-source platform for biological-image analysis, Nat. Methods 9 (2012) 676–682, https://doi.org/10.1038/nmeth.2019.
[28] K. Yvon, W. Jeitschko, E. Parthé, LAZY PULVERIX, a computer program for calculating X-ray and neutron diffraction powder patterns, J. Appl. Crystallogr. 10 (1977) 73–74, https://doi.org/10.1107/S0021889877012898.
[29] S. DeMeo, Does copper metal react with acetic acid? J. Chem. Educ. 74 (7) (1997) 844–846, https://doi.org/10.1021/ed074p844.
[30] V.B. Singh, R.N. Singh, Corrosion and inhibition studies of copper in aqueous solutions of formic acid and acetic acid, Corros. Sci. 37 (9) (September 1995) 1399–1410, https://doi.org/10.1016/0010-938X(95)00042-I.
[31] G. Kilinççeker, H. Galip, The effects of acetate ions (CH3COO−) on electrochemical behavior of copper in chloride solutions, Mater. Chem. Phys. 110 (2–3) (2008) 380–386, https://doi.org/10.1016/j.matchemphys.2008.02.026.